

DVCS at HERMES: Recent Results

F. Ellinghaus*

*University of Colorado,
Department of Physics,
Boulder, Colorado 80309-0390, USA
E-mail: Frank.Ellinghaus@desy.de*

for the HERMES Collaboration

Hard exclusive reactions are the tool to learn about generalized parton distributions, which provide a more complete parametrization of the nucleon than the ordinary parton distribution functions. Recent measurements by the HERMES collaboration of the exclusive production of photons, i.e., Deeply-Virtual Compton Scattering, are summarized and compared to model calculations, focusing on the measurements and model comparisons relevant to the extraction of quark orbital angular momentum and on the measurements on heavy nuclei.

Keywords: DVCS, exclusive reactions, GPD, angular momentum, proton

1. Introduction

Similar to the case of inclusive and semi-inclusive DIS, where the nucleon structure is described using **P**arton **D**istribution **F**unctions (PDFs), hard exclusive reactions can be expressed in terms of **G**eneralized **P**arton **D**istributions (GPDs).¹⁻³ The PDFs and elastic nucleon **F**orm **F**actors (FFs) are included in the GPDs as the limiting cases and moments of GPDs, respectively.² While FFs derived in elastic scattering describe the transverse location of partons inside the nucleon and PDFs describe their longitudinal momentum distribution, GPDs are able to provide information on both at the same time. Thus exclusive reactions are able to give a certain 3-dimensional picture of the nucleon structure.⁴⁻⁶ In particular, GPDs offer for the first time a possibility to determine the total angular momentum carried by the quarks in the nucleon.²

Below recent HERMES measurements on the hard exclusive electropro-

*This work is supported in part by the US Department of Energy.

duction of real photons (**D**eeply-**V**irtual **C**ompton **S**cattering, DVCS) are summarized and compared to model calculations. The data has been taken with polarized and unpolarized gas targets using the HERMES spectrometer⁷ at the HERA electron/positron-proton collider at DESY, which offers longitudinally polarized 27.6 GeV electron and positron beams.

2. GPD H via beam-charge and beam-spin asymmetries

DVCS amplitudes can be measured through the interference between the DVCS and **B**ethe-**H**eitler (BH) processes, in which the photon is radiated from a parton in the former and from the electron in the latter process. Both processes have an identical final state, i.e., they are indistinguishable, and thus give rise to an interference term I . The photon production cross section depends on the Bjorken scaling variable x_B , the squared virtual-photon four-momentum $-Q^2$, the squared four-momentum transfer t or the reduced four-momentum transfer $t' = (t - t_{min})$ to the target, and the azimuthal angle ϕ defined as the angle between the lepton scattering plane and the (virtual and real) photon production plane. For an unpolarized proton target, and at leading twist, the interference term is given by⁸

$$I \propto -C [a \cos \phi \operatorname{Re} \mathcal{M}^{1,1} - b P_l \sin \phi \operatorname{Im} \mathcal{M}^{1,1}], \quad (1)$$

where the lepton beam has longitudinal polarization P_l and charge $C = \pm 1$, and a and b are functions of the ratio of the longitudinal to transverse virtual-photon flux. The real (imaginary) part of the DVCS amplitude $M^{1,1}$ can be accessed by measuring the $\cos \phi$ ($\sin \phi$) dependence of a cross section asymmetry with respect to the charge (spin) of the lepton beam. At HERMES kinematics, the DVCS amplitude $M^{1,1}$ gives access to the GPD H . Details and full equations are given in Ref. 9.

The event selection at HERMES requires events with exactly one photon and one charged track, identified as the scattered lepton, with $Q^2 > 1 \text{ GeV}^2$. For data taken prior to 2006 the recoiling proton is not detected and exclusive events are identified by the fact that the missing mass M_x of the reaction $ep \rightarrow e\gamma X$ corresponds to the proton mass. Due to the finite energy resolution the exclusive sample is defined as $-1.5 < M_x < 1.7 \text{ GeV}$. A recoil detector used during the recent data taking should reduce the underlying background from presently about 15% to less than 1%.¹⁰

The beam-spin asymmetry (BSA) and the beam-charge asymmetry (BCA) as a function of ϕ are calculated as

$$A_{LU}(\phi) = \frac{1}{\langle |P_l| \rangle} \frac{\vec{N}(\phi) - \overleftarrow{N}(\phi)}{\vec{N}(\phi) + \overleftarrow{N}(\phi)}, \quad A_C(\phi) = \frac{N^+(\phi) - N^-(\phi)}{N^+(\phi) + N^-(\phi)}, \quad (2)$$

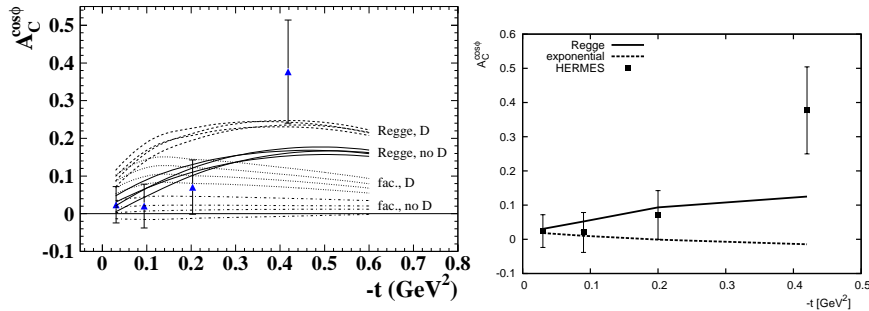


Fig. 1. The $\cos\phi$ amplitude of the beam-charge asymmetry¹² on hydrogen as a function of $-t$. The error bars show the statistical and systematic uncertainties added in quadrature. The calculations in the left panel are based on a double-distribution GPD model using a factorized (fac.) or a Regge-inspired (Regge) t -dependence with (D) or without (no D) a D-term contribution. The parameters b_v and b_s are each set to either unity or infinity. Using the resulting 16 sets of model parameters, the calculated asymmetries fall into four main groups. The variations within these groups are due to the different settings for the b parameters. The calculations in the right panel are based on a dual-parametrization GPD model.¹⁸

with the normalized yields \vec{N} (\overleftarrow{N}) or N^+ (N^-) using a beam with positive (negative) helicity or a positron (electron) beam, respectively. The BSA (BCA) on the proton as a function of ϕ has been extracted at HERMES¹¹ (¹²), whereby the predominant $\sin\phi$ ($\cos\phi$) dependence expected from Eqn. 1 has been observed. The $\cos\phi$ amplitudes of the BCA on hydrogen as a function of $-t$ derived from a fit to the BCA in each $-t$ bin¹² are shown in Fig.1, and the recent preliminary BSA result on the kinematic dependences of the $\sin\phi$ amplitudes is shown in Fig.2.

The model calculations shown in the left panel (left column) of Fig.1 (Fig.2) are based on a double-distribution GPD model described in Refs. 13,14. Since these data are exclusively sensitive to the GPD H as mentioned above, the theoretical calculations shown were derived by only varying the model parameters for the GPD H in the underlying code¹⁵ in order to calculate the asymmetries at the average kinematics of every bin. The model parameters differ with respect to including or neglecting the so-called D-term¹⁶ in the GPD model and whether the t -dependence of the GPD H is calculated in either the simplest ansatz where the t -dependence factorizes from the t -independent part or in the Regge-motivated ansatz. In addition, the so-called skewness parameters b_v and b_s in the profile function¹⁷ have been set to either unity or infinity, the latter value corresponds to a skewness

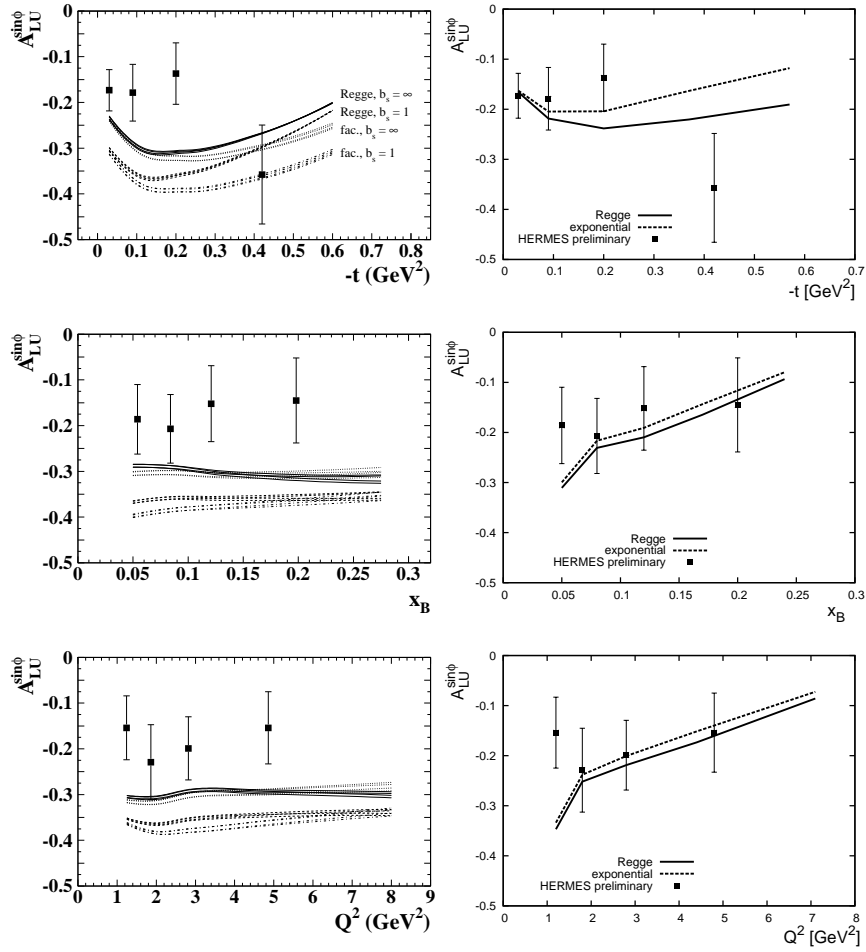


Fig. 2. The $\sin \phi$ amplitude of the beam–spin asymmetry on hydrogen from the 1996–2000 data as a function of $-t$, x_B and Q^2 . The error bars show the statistical and systematic uncertainties added in quadrature. The calculations in the left panel are based on a double-distribution GPD model using a factorized (fac.) or a Regge–inspired (Regge) t –dependence with or without a D–term contribution. The parameters b_v and b_s are each set to either unity or infinity. Using the resulting 16 sets of model parameters, the calculated asymmetries fall into four main groups, whereby the BSA appears to be insensitive to the D–Term and to the value of b_v . The calculations in the right column are based on a dual-parametrization GPD model.¹⁸

independent ansatz for the GPD. The BCA data appears to disfavor the four parameters sets with the Regge–inspired t –dependence and the D–term

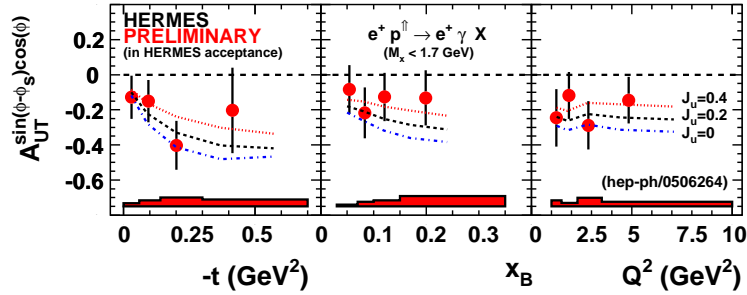


Fig. 3. The $\sin(\phi - \phi_S) \cos \phi$ amplitude of the transverse target-spin asymmetry as a function of $-t$, x_B and Q^2 in comparison to theoretical predictions from Ref. 20.

contribution as well as the factorized one with the D-term which gives the largest asymmetry ($b_v = 1$, $b_s = \infty$). For the BSA all models seem to overshoot the absolute size of the $\sin \phi$ amplitude. The calculations based on the dual parametrization GPD model¹⁸ shown in the right panel (right column) of Fig.1 (Fig.2) are all in rather good agreement with the data.

3. GPDs H and E via transverse target-spin asymmetry

Within the next few years HERMES will be able to provide sufficient data to largely constrain the GPD H in the kinematic region of the experiment. It is natural to ask to what extent the GPD E can be accessed, which is the other important GPD necessary in order to determine J_q , the total orbital angular momentum of quarks in the nucleon.² For an unpolarized proton target the contribution from the GPD E is suppressed with respect to H , but this is different for transverse target polarization.^{9,19} Using an unpolarized beam (U) and a transversely (T) polarized target, a $\sin(\phi - \phi_S) \cos \phi$ modulation in the DVCS transverse target-spin asymmetry (TTSA) gives access to a combination of the GPDs H and E .²⁰ Here ϕ_s denotes the azimuthal angle of the target polarization vector with respect to the lepton scattering plane.

The results from HERMES data collected on a transversely polarized hydrogen target are shown in Fig. 3. They agree with the model calculations²⁰ shown in the same figure, which have been calculated for various values of J_u . Based on u -quark dominance the d -quark total angular momentum has been assumed to be zero. Since it was realized that the model calculations are largely insensitive to all model parameters but J_u and J_d , it is possible to constrain J_u and J_d even though other model parameters are largely unconstrained.²⁰ For example, the model calculations in Fig. 3 show

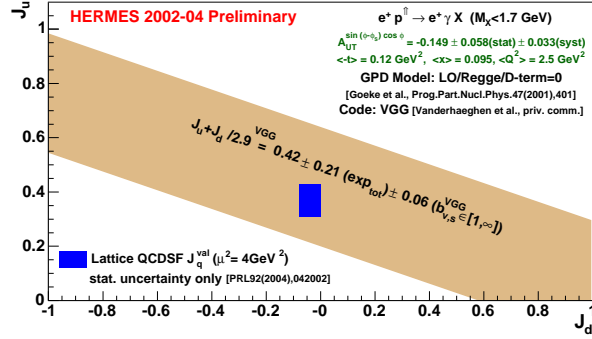


Fig. 4. Model dependent constraint on the quark orbital angular momenta J_u and J_d .

little variation if calculated for any of the 16 parameter sets which give very different values for the BCA as shown in Fig.1. Hence the four parameter sets with the Regge-inspired t -dependence and without a contribution of the D-term (solid lines in the left panel of Fig.1), have been chosen in order to determine the parameter space allowed for J_u and J_d . For different values of J_u and J_d these sets have been compared to the DVCS TTSA data shown in Fig. 3, leading to a first model dependent constraint on J_u versus J_d shown in Fig.4.²¹ Further improvement can be expected, taking into account that the GPD H and therefore the available theoretical models will be well constrained by the upcoming HERMES data, and that the data shown here is less than half of the data taken on the transversely polarized hydrogen target. Due to the good agreement between the calculations in the dual-parametrization model and the BSA and BCA results as shown above, the next natural step is to also calculate the allowed parameter space for J_u and J_d within this model. This effort is presently ongoing, but calculations for various values of J_u at a fixed $J_d = 0$ ¹⁸ already indicate that the dual model favors smaller values for J_u than the double-distribution one.

4. DVCS on Nuclei

Beam-Spin Asymmetries have also been measured on deuterium and various heavier nuclei (He, N, Ne, Kr, Xe). Coherent processes are dominant for small values of $-t$, while at larger values incoherent scattering on the individual protons and neutrons dominates. Based on MC studies a region of small $-t'$ ("coherent enriched") has been selected for each nucleus in order to have similar average kinematic values for all targets ($\langle -t' \rangle = 0.018$

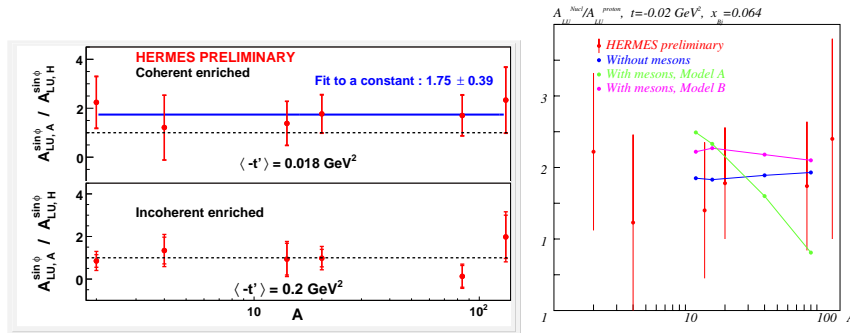


Fig. 5. The $\sin\phi$ amplitude of the BSA on D, He, N, Ne, Kr, Xe divided by the one on the proton in two different kinematic regions dominated by either coherent or incoherent processes (left panel). The 'coherent enriched' result (left panel, upper row) is compared to model calculations²⁶ in the right panel.

GeV^2 , $\langle Q^2 \rangle \approx 1.7 \text{ GeV}^2$, $\langle x_B \rangle \approx 0.065$). According to the MC studies the fraction of coherent processes is approximately 82% for all but the lighter targets (D, He). Similarly, an "incoherent enriched" sample has been selected with an average $-t'$ of 0.2 GeV^2 . The ratio of the BSA on the nuclei divided by the one on the proton at the same average kinematics is shown in the left panel of Fig.5. A simple fit to a constant for the coherent enriched sample yields a value above unity by two sigma, while the incoherent enriched sample shows asymmetries very similar to the one on the proton. Note that this is in agreement with earlier HERMES preliminary results²² where a value consistent with unity was found when comparing the BSA on deuterium and neon to the one on the proton in the full t range. The BSAs on nuclei are expected to be similar to the one on the proton in the incoherent enriched sample since scattering on the protons inside the nuclei should dominate due to the fact that the BH process on the neutron is suppressed. The fit value found for the coherent enriched sample is consistent with a very basic prediction of 5/3 for Spin-0 and Spin-1/2 targets, based on the ratio of the involved valence-quark charges squared,²³ as well as with calculations done specifically for neon and krypton.²⁴ Also a prediction of $R = 1-1.1$ for Helium²⁵ is in agreement with the measurement. The result of a recent calculation²⁶ is shown in the right panel of Fig.5, whereby one of the three models is disfavored by the data.

5. Summary

The HERMES DVCS data on beam-charge and beam-spin asymmetries is already able to distinguish between some GPD models. Based on a certain model, the DVCS measurements on transversely polarized hydrogen lead to a first model dependent constraint for the total angular momentum of quarks in the nucleon. This method, together with increased statistics and improved models should allow for a constraint with reasonable statistical and theoretical uncertainties in the future.

References

1. D. Müller et al., *Fortschr. Phys.* **42** (1994) 101.
2. X. Ji, *Phys. Rev. Lett.* **78** (1997) 610, *Phys. Rev.* **D55** (1997) 7114.
3. A.V. Radyushkin, *Phys. Lett.* **B380** (1996) 417, *Phys. Rev.* **D56** (1997) 5524.
4. M. Burkardt, *Phys. Rev.* **D62** (2000) 071503; Erratum-*ibid.* **D66** (2002) 119903.
5. A.V. Belitsky and D. Müller, *Nucl. Phys.* **A711** (2002) 118.
6. J.P. Ralston and B. Pire, *Phys. Rev.* **D66** (2002) 111501.
7. HERMES Coll., K. Ackerstaff et al., *Nucl. Instr. and Meth.* **A417** (1998) 230.
8. M. Diehl et al., *Phys. Lett.* **B411** (1997) 193.
9. A.V. Belitsky, D. Müller and A. Kirchner, *Nucl. Phys.* **B629** (2002) 323.
10. R. Perez-Benito, these proceedings.
11. HERMES Coll., A. Airapetian et al., *Phys. Rev. Lett.* **87** (2001) 182001.
12. HERMES Coll., A. Airapetian et al., *Phys. Rev.* **D75** (2007) 011103.
13. M. Vanderhaeghen, P.A.M. Guichon and M. Guidal, *Phys. Rev.* **D60** (1999) 094017.
14. K. Goeke, M.V. Polyakov and M. Vanderhaeghen, *Prog. Part. Nucl. Phys.* **47** (2001) 401.
15. M. Vanderhaeghen, P.A.M. Guichon and M. Guidal, Computer code for the calculation of DVCS and BH processes, Private Communication, 2001.
16. M.V. Polyakov and C. Weiss, *Phys. Rev.* **D60** (1999) 114017.
17. I.V. Musatov and A.V. Radyushkin, *Phys. Rev.* **D61** (2000) 074027.
18. V. Guzey and T. Teckentrup, *Phys. Rev.* **D74** (2006) 054027.
19. M. Diehl, *Phys. Rept.* **388** (2003) 41.
20. F. Ellinghaus, W.-D. Nowak, A.V. Vinnikov and Z. Ye, *Eur. Phys. J.* **C46** (2006) 729.
21. HERMES Coll., Z. Ye, Proceedings of 14th International Workshop on Deep Inelastic Scattering (DIS 2006), Tsukuba, Japan, hep-ex/0606061.
22. HERMES Coll., F. Ellinghaus et al., Proceedings of the 15th International Spin Physics Symposium (Spin 2002), Upton, New York, AIP Conf. Proc. **675** (2002) 303, hep-ex/0212019.
23. A. Kirchner and D. Müller, *Eur. Phys. J.* **C32** (2003) 347.
24. V. Guzey and M. Strikman, *Phys. Rev.* **C68** (2003) 015204.
25. S. Liuti and S.K. Taneja, *Phys. Rev.* **C72** (2005) 032201.
26. V. Guzey and M. Siddikov, *J. Phys.* **G32** (2006) 251.